



Wang, X., Jiang, Z., Zhang, K., Wen, M., Xue, Z., Wu, W., Huang, Y., Wang, Q., Liu, X., Liu, T., & Xie, X. (2020). Analysis of gas composition and nitrogen sources of shale gas reservoir under strong tectonic events: Evidence from the complex tectonic area in the yangtze plate. *Energies*, 13(1), [281].  
<https://doi.org/10.3390/en13010281>

Publisher's PDF, also known as Version of record

License (if available):  
CC BY

Link to published version (if available):  
[10.3390/en13010281](https://doi.org/10.3390/en13010281)

[Link to publication record in Explore Bristol Research](#)  
PDF-document

This is the final published version of the article (version of record). It first appeared online via MDPI at <https://www.mdpi.com/1996-1073/13/1/281>. Please refer to any applicable terms of use of the publisher.


## University of Bristol - Explore Bristol Research

### General rights

This document is made available in accordance with publisher policies. Please cite only the published version using the reference above. Full terms of use are available:  
<http://www.bristol.ac.uk/red/research-policy/pure/user-guides/ebr-terms/>

## Article

# Analysis of Gas Composition and Nitrogen Sources of Shale Gas Reservoir under Strong Tectonic Events: Evidence from the Complex Tectonic Area in the Yangtze Plate

Xin Wang <sup>1,2</sup>, Zhenxue Jiang <sup>1,2,\*</sup>, Kun Zhang <sup>3,4,\*</sup> , Ming Wen <sup>1,2,5</sup>, Zixin Xue <sup>1,2</sup>, Wei Wu <sup>6</sup>, Yizhou Huang <sup>1,2,7</sup>, Qianyou Wang <sup>1,2</sup>, Xiaoxue Liu <sup>1,2</sup>, Tianlin Liu <sup>1,2</sup> and Xuelian Xie <sup>8</sup>

<sup>1</sup> State Key Laboratory of Petroleum Resources and Prospecting, China University of Petroleum, Beijing 102249, China; wangxin\_cup@163.com (X.W.); mingw930331@163.com (M.W.); 2018310203@student.cup.edu.cn (Z.X.); ejeo33@163.com (Y.H.); 2016210217@student.cup.edu.cn (Q.W.); iris\_1314\_iris@163.com (X.L.); 2015210204@student.cup.edu.cn (T.L.)

<sup>2</sup> Unconventional Natural Gas Institute, China University of Petroleum, Beijing 102249, China

<sup>3</sup> School of Geoscience and Technology, Southwest Petroleum University, Chengdu 610500, China

<sup>4</sup> State Key Laboratory of Oil and Gas Reservoir Geology and Exploitation, Southwest Petroleum University, Chengdu 610500, China

<sup>5</sup> WA School of Mines: Minerals, Energy and Chemical Engineering, Curtin University, Perth, WA 6102, Australia

<sup>6</sup> Shale Gas Research Institute, PetroChina Southwest Oil & Gas Field Company, Chengdu 610500, China; wuwei06@petrochina.com.cn

<sup>7</sup> Organic Geochemistry Unit, School of Chemistry, University of Bristol, Cantock's Close, Bristol BS8 1TS, UK

<sup>8</sup> Guangzhou Marine Geological Survey, Guangzhou 510760, China; 15652635334@163.com

\* Correspondence: jiangzx@cup.edu.cn (Z.J.); 201999010133@swpu.edu.cn (K.Z.)

Received: 13 November 2019; Accepted: 3 January 2020; Published: 6 January 2020



**Abstract:** Strong tectonic movement brings great risk to exploration of shale gas in southern China, especially in Lower Cambrian shale with complex tectonic backgrounds, which has good hydrocarbon-generation matter but low or no gas content. In this paper, the Lower Cambrian shale from the southeast Chongqing region, located in the Upper Yangtze Platform, and the Xiuwu Basin, located in the Lower Yangtze Platform, were selected as the research objects. First, the gas components in shale gas samples were measured, then analysis of nitrogen isotopic was used to reveal the nitrogen sources. Using regional geological backgrounds, core description, and seismic interpretation, combined with the perpendicular and parallel permeability test and focused ion beam–helium ion microscopy (FIB–HIM) observation, the reasons for high content of nitrogen in the Lower Cambrian shale from the Xiuwu Basin and the Southeast Chongqing region were clarified. The results indicate that the main sources of nitrogen in the Lower Cambrian shale gas at the Southeast Chongqing region is the thermal evolution of organic matter and atmosphere. Nitrogen in the atmosphere is filled into the shale reservoir through migration channels formed by detachment layers at the bottom of the Lower Cambrian, shale stratification planes, and widespread thrust faults. Nitrogen was also produced during the thermal evolution of organic matter. Both are responsible for the low content of hydrocarbon and high content of nitrogen of shale gas in the Southeast Chongqing region. Further, the main sources of nitrogen in the Lower Cambrian shale gas at the Xiuwu Basin is the upper mantle, superdeep crust, and atmosphere. Nitrogen in the atmosphere is also filled into the shale reservoir through migration channels formed by detachment layers at the bottom of the Lower Cambrian, shale stratification planes, and widespread thrust faults. Nitrogen was also produced by volcanism during the Jurassic. Both are the causes of the low content of hydrocarbon and high content of nitrogen in shale gas in the Xiuwu Basin. Finally, destruction models for shale gas reservoirs

with complex tectonic backgrounds were summarized. This research aimed to provide a theoretical guidance for shale gas exploration and development in areas with complex tectonic backgrounds.

**Keywords:** nitrogen isotope; atmospheric source; thermal evolution of organic matter; deep crust-upper mantle source; stratification planes; detachment layers; deep fault; volcanic activity

---

## 1. Introduction

Shale gas has become an important natural gas resource. In recent years, due to the development of geological understanding, organic-rich shale has become a hot target for natural gas exploration and development around the world [1–3]. At the same time, application of horizontal well technology and hydraulic fracturing has greatly boosted the production efficiency of shale gas [4–8]. In China, a number of shale gas blocks were built successively and achieved large-scale development by 2018, namely Weiyuan, Fushun–Yongchuan, Changning, Dingshan, and Jiaoshiba [9,10]. However, compared with the Paleozoic marine shale in North America, marine shale in southern China underwent complex process of thermal evolution and multistage tectonic movements. Although marine shale in the South China plate has little variation in terms of mineral composition and total organic carbon (TOC) content, there are great differences in gas composition due to diverse sealing conditions in different regions and layers. Nitrogen is common component of natural gas. Natural gas reservoirs with high nitrogen content are found in many oil-bearing basins around the world. In the gas fields of the United States, the average nitrogen content is 3%. The nitrogen content is lower than 5% in most of the natural gas reservoirs in the Ordos Basins and Sichuan Basins of China [11]. The content of nitrogen in natural gas stays in the range of 10–30% in the Tarim Basin [12,13], and in the Fuling block in the Sichuan Basin, shale gas contains almost nitrogen-free [14,15]. High nitrogen content of natural gas not only brings great risks for oil and gas exploration, but also causes a series of difficult problems for resource evaluation and development [16,17]. Therefore, it becomes an important problem to solve shale gas composition with complex tectonic backgrounds and precisely select favorable areas [18].

A series of studies on correlation between tectonic movement and shale gas accumulation was carried out previously. Kang et al. (2017) studied shale gas enrichment conditions in areas with complex tectonic backgrounds by taking the front of Daba Mountain in the northern margin of the Sichuan Basin as an example. The authors found that good sealing conditions play a key role in shale gas enrichment in this area, and that the sealing conditions are influenced by widely developed deep faults and inclined folds broken by faults [19]. Considering the structural features in the front of Daba Mountain and the influence of burial depth, less-developed fractures in the delamination belts near the basin, widely distributed synclines and anticlines, and relatively wide and gentle boxlike anticlines in this area were considered as the targets of exploration. Hu et al. (2017) analyzed the structural characteristics of the block in the Fuling shale gas field of the Sichuan Basin and clarified the main structural factors affecting the productivity of shale gas wells by different structural units [20]. The results showed that the influence of structural characteristics on shale gas production capacity is reflected in the fracturing effects and gas-bearing property. The stronger the structural deformation, the more developed the fractures, and the greater the burial depth and negative compressive stress, the worse the fracturing effect. On the other hand, the lesser the burial depth and negative compressive stress, the better the fracturing effect. The stronger the structural deformation, the larger the large-scale fracture, and the higher the degree of natural fracture development, the easier it is for the shale gas to escape and the lower the gas content; otherwise, the higher the gas content. After analyzing the main controlling factors the accumulation of the Fuling shale gas field, Guo et al. (2017) believed that the sealing conditions determined by the duration and strength of later tectonic processes were the key geological factors for reservoir formation and the production of shale gas, and that a good shale floor and roof can effectively limit vertical dispersion of hydrocarbon [9]. In this case, the shale reservoir has

high porosity, high gas content, and high pressure, which are beneficial to the formation of a high-yield region for shale gas.

Some shale gas blocks located outside the stable basin, such as the Xiuwu Basin and the Southeast Chongqing region, have good hydrocarbon-generation matter. However, commercially valuable shale gas reservoirs have not been found in these blocks, and the exploration wells have shown that the nitrogen content in these blocks is far higher than in other shale gas blocks, illustrating that the characteristics of the Lower Cambrian shale gas reservoir in these blocks are distinct from those of shale gas blocks with high methane content. Based on the geochemical characteristics of the Lower Cambrian shale gas in the typical complex tectonic zone from the Yangtze Plate, such as the Xiuwu Basin and Southeast Chongqing region, this study used nitrogen isotopes to trace the sources of nitrogen and then considered regional geological backgrounds and tectonic deformation characteristics to analyze the reasons for low hydrocarbon and high nitrogen. Finally, destruction models for shale gas reservoirs were established in these blocks, which provide a scientific basis for guiding the exploration and development of highly evolved shale gas in complex tectonic areas.

## 2. Geological Setting

### 2.1. Tectonic Characteristics

The scope of this research was the whole Yangtze region. The primitive continental crust of southern China was separated into two ancient plates, the Yangtze and Cathaysian, in the early period of the Mesoproterozoic Era [21–23]. During the Early Cambrian, the two plates were extended with the occurrence of large-scale transgression, resulting in the deposition of a set of organic-rich shale across almost all of the Yangtze plate. Then, the water body began to shallow. In this case, the lithologic features of the Yangtze plate changed from fine-grained and silty shale to siltstone, sandstone, and other coarse-grained clastic rocks. The collision between the Yangtze and Cathaysian plates in the Ordovician period caused the water body to continue to become shallow, in which the sedimentary system on the Yangtze plate transformed from clastic to carbonate. In the Silurian period, a transgression occurred, causing the sedimentary system to change back to a clastic sedimentary system. During this period, the oceanic basin between the two plates was subjected to gradual subduction and collision toward the Yangtze Plate. By the Late Silurian period, the Yangtze and Cathaysian Plates merged into one, namely the uniform South China Plate. The Xiuwu Basin and the Southeast Chongqing region are representative blocks with complex tectonic backgrounds, both of which are located outside the large stable sedimentary basins. Southeast Chongqing region is located on the southeast side of Sichuan Basin (Figure 1A,D), and Xiuwu Basin is located on the southeast side of Jiangnan Basin (Figure 1C,F). Southeastern Chongqing borders Sichuan Basin. The distance between Xiuwu Basin and Jiangnan Basin is about 60 kilometers. The two blocks are not far from the junction of the two plates and experienced intense tectonic movement against complex tectonic backgrounds.

### 2.2. Sedimentary and Stratum Characteristics

During the Early Cambrian, the sedimentary environments on the Yangtze plate from northwest to southeast were ancient lands, a shallow shelf, a deep shelf, a continental slope, and an ocean basin [24,25], as shown in Figure 1G. The target layer for this research was a set of shale that was widely deposited on the Yangtze plates in the Early Cambrian. Because of the widespread distribution of shale, they are called different names in various regions. In the Upper Yangtze area, they are known as the Qiongzhusi Formation, while in the Sichuan Basin and outside of the Sichuan Basin (such as the Southeast Chongqing region), they are called the Niutitang Formation. In the Lower Yangtze area, they are known as the Wangyinpu and Guanyintang Formations, which are sets of black to deep gray organic-rich siliceous shale deposited early in the Early Cambrian and the key target strata for China's shale gas exploration.

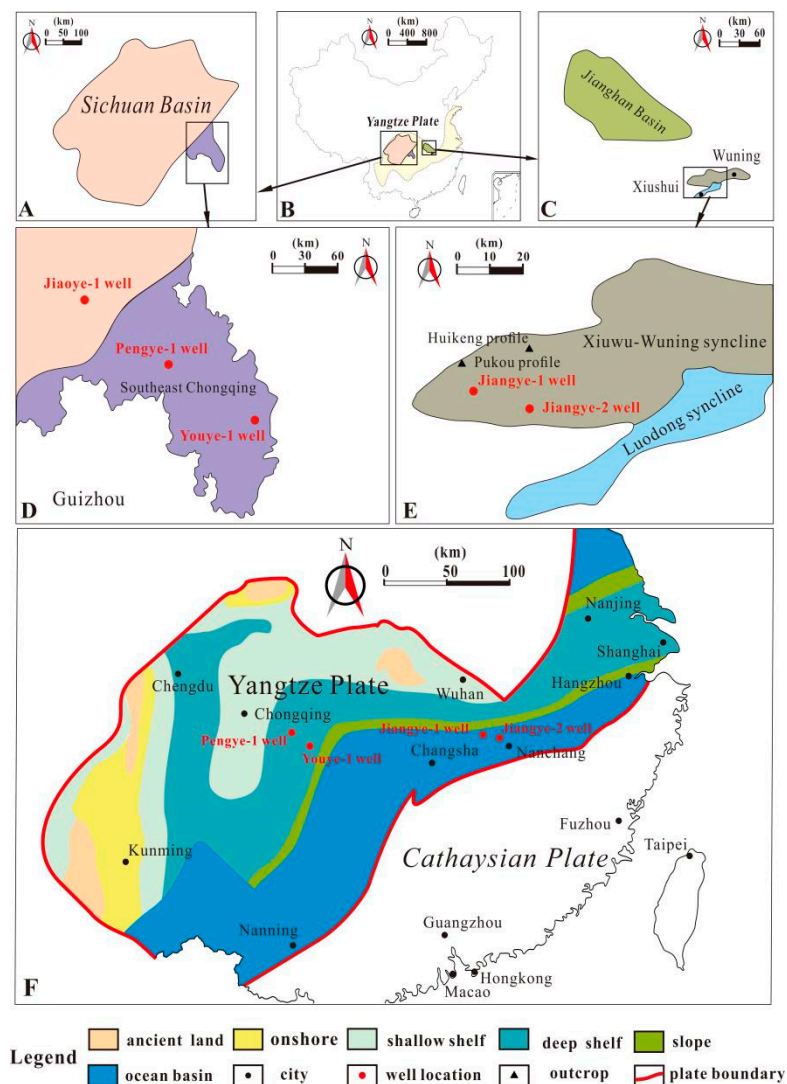


**Figure 1.** Geological maps of the research areas. (A,D) Geographical location maps of Southeast Chongqing. Pengye-1 and Youye-1 wells are located in this block, and Jiaoye-1 well is located in the Sichuan Basin. (B) Geographical location map showing Southeast Chongqing region in Upper Yangtze area and Xiuwu Basin in Lower Yangtze area. (C,E) Geographical location maps of Xiuwu Basin. Jiangye-1 and Jiangye-2 wells are located in this block, which is closest to the junction of the Yangtze and Cathaysian plates. (F) Map of sedimentary features of Yangtze plate in Early Cambrian.

### 3. Samples, Experiment, and Data Sources

#### 3.1. Gas Composition and Nitrogen Isotope Test

The Shimadzu GC-2014 gas chromatograph (JPN) was used for quantitative multicomponent analysis of mixed gases in this study. The stainless-steel chromatographic column was placed in a room with a constant temperature of 60 °C. The six-way valve sample injector used a sample loop with a capacity of 1 mL, and the temperature was kept constant at 100 °C. The thermal conductivity cell detector was kept under a constant temperature of 200 °C. Nitrogen isotope tests were used to determine the source of nitrogen, implemented with an EA IsoLink Plus EA-IRMS device using helium (99.999%) as the carrier gas at a flow rate of 1.3 mL/min. The gas sample feeding was implemented in a split-stream sampling approach (with a split ratio of 20:1) with a gas inlet temperature of 200 °C. Specifically, the temperature was held at 35 °C for 6 min, then increased to 80 °C at a rate of 15 °C/min and 200 °C at a rate of 5 °C/min, and finally held constant at 200 °C for 5 min. The reacting furnace

temperature was 940 °C. Eight shale gas samples were taken from the Niutitang Formation in the Youye-1 well and 16 from the Wangyinpu and Guanyintang Formations in Xiuwu Basin. The shale gas sample information can be seen in Table 1.

**Table 1.** Experimental numbers, wells, geologic age, and formation names of gas samples. The well locations can be seen in Figure 1.

Number	Well	Geologic Age	Formation
1	Youye-1	Early Cambrian	Niutitang
2	Youye-1	Early Cambrian	Niutitang
3	Youye-1	Early Cambrian	Niutitang
4	Youye-1	Early Cambrian	Niutitang
5	Youye-1	Early Cambrian	Niutitang
6	Youye-1	Early Cambrian	Niutitang
7	Youye-1	Early Cambrian	Niutitang
8	Youye-1	Early Cambrian	Niutitang
9	Jiangye-1	Early Cambrian	Guanyintang
10	Jiangye-1	Early Cambrian	Guanyintang
11	Jiangye-1	Early Cambrian	Guanyintang
12	Jiangye-1	Early Cambrian	Guanyintang
13	Jiangye-1	Early Cambrian	Guanyintang
14	Jiangye-1	Early Cambrian	Guanyintang
15	Jiangye-1	Early Cambrian	Guanyintang
16	Jiangye-1	Early Cambrian	Guanyintang
17	Jiangye-1	Early Cambrian	Guanyintang
18	Jiangye-1	Early Cambrian	Guanyintang
19	Jiangye-1	Early Cambrian	Wangyinpu
20	Jiangye-1	Early Cambrian	Wangyinpu
21	Jiangye-1	Early Cambrian	Wangyinpu
22	Jiangye-1	Early Cambrian	Wangyinpu
23	Jiangye-1	Early Cambrian	Wangyinpu
24	Jiangye-1	Early Cambrian	Wangyinpu

### 3.2. Experiment of Permeability Perpendicular and Parallel to Stratification Plane

The traditional steady-state test technology mainly uses Darcy's law to calculate permeability based on the gas flow rate per unit time under the condition of stable pressure difference, which makes the permeability measured higher under low average pressure and lower under high average pressure. Therefore, the Klinkenberg correction of data is necessary in permeability tests [26–28]. The non-steady-state pulse attenuation permeability measurement technology can avoid the gas flow measurement and calculate permeability by the pressure difference–time curve of the core front and back to weaken the gas slip effect [29]. The permeability of the shale samples was measured perpendicular and parallel to the stratification planes with a PDP-200 pulse decay permeability analyzer (USA). Since gas slippage is more evident in shales under low pore pressure [28], the permeability of the shale samples was tested at 1000 psi. This study collected 16 shale samples from the Lower Yangtze area. Before the test, the shale samples were made into cylinders with a length of 50 mm and a diameter of 25 mm. We also collected test results for 12 samples from the Upper Yangtze area [30]. The gas sample information is shown in Table 2.

### 3.3. FIB–HIM Experiment

Focused ion beam–helium ion microscopy (FIB–HIM) contains three parts: The cutting function of a focused ion beam (FIB), the imaging function of a helium ion microscope (HIM), and a neon (Ne) ion beam. Compared with a field emission scanning electron microscope (FE–SEM), a scanning helium ion microscope has higher resolution, which makes it easier to distinguish micro–nanopore in shale. Before sample observation, FIB–HIM samples must be ground and Ar-ion polished. In this research,



a NanoFab ORION microscope was used to observe an organic-rich shale sample from the Niutitang Formation at 3811 m in the Youye-1 well, and experimental images of organic-rich shale samples were taken from the Longmaxi Formation at 2402 m in the Jiaoye-1 well [31].

**Table 2.** Experimental numbers, wells, geologic age, and formation names of core samples. The well locations can be seen in Figure 1.

Number	Well	Geologic Age	Formation
1	Jiangye-1	Early Cambrian	Guanyintang
2	Jiangye-1	Early Cambrian	Wangyinpu
3	Jiangye-1	Early Cambrian	Wangyinpu
4	Jiangye-2	Early Cambrian	Guanyintang
5	Jiangye-2	Early Cambrian	Guanyintang
6	Jiangye-2	Early Cambrian	Guanyintang
7	Jiangye-2	Early Cambrian	Guanyintang
8	Jiangye-2	Early Cambrian	Guanyintang
9	Jiangye-2	Early Cambrian	Wangyinpu
10	Jiangye-2	Early Cambrian	Wangyinpu
11	Jiangye-2	Early Cambrian	Wangyinpu
12	Jiangye-2	Early Cambrian	Wangyinpu
13	Jiangye-2	Early Cambrian	Wangyinpu
14	Jiangye-2	Early Cambrian	Wangyinpu
15	Jiangye-2	Early Cambrian	Wangyinpu
16	Jiangye-2	Early Cambrian	Wangyinpu
17	Pengye-1	Early Silurian	Longmaxi
18	Pengye-1	Early Silurian	Longmaxi
19	Pengye-1	Early Silurian	Longmaxi
20	Pengye-1	Early Silurian	Longmaxi
21	Pengye-1	Early Silurian	Longmaxi
22	Pengye-1	Early Silurian	Longmaxi
23	Pengye-1	Early Silurian	Longmaxi
24	Pengye-1	Early Silurian	Longmaxi
25	Pengye-1	Early Silurian	Longmaxi
26	Pengye-1	Early Silurian	Longmaxi
27	Pengye-1	Early Silurian	Longmaxi
28	Pengye-1	Early Silurian	Longmaxi

## 4. Results and Discussion

### 4.1. Shale Gas Composition and Nitrogen Isotope Analysis

#### 4.1.1. Shale Gas Composition Analysis

According to gas composition analysis of eight gas samples from the Niutitang Formation in the Youye-1 well and 16 gas samples from the Wangyinpu and Guanyintang Formations in the Jiangye-1 well, the experimental results show that the gas composition was mainly composed of  $O_2$  and  $N_2$ , as shown in Figure 2A,B. Counter art average volume percentages were 11% and 83%, in the Youye-1 well and 17% and 80% in the Jiangye-1 well. These values are close to the proportions of  $O_2$  and  $N_2$  in atmosphere (21% and 78%, respectively). The average content of methane was lower than 1% in the two wells.

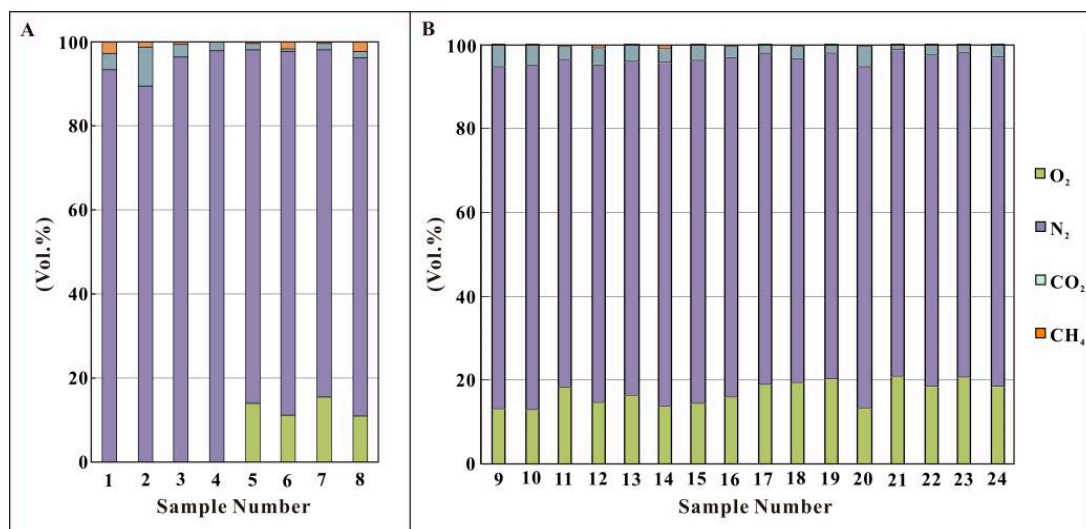


**Figure 2.** Results of gas composition analysis: (A) Niutitang Formation gas samples from the Youye-1 well; (B) Wangyinpu and Guanyintang Formations gas samples from the Jiangye-1 well. The gas sample information can be seen in Table 1.

#### 4.1.2. Nitrogen Isotope Analysis

The results of nitrogen isotope analysis of the Niutitang Formation gas samples from the Youye-1 well and the Wangyinpu and Guanyintang Formation gas samples from the Jiangye-1 well are shown in Figure 3A,B. In the Youye-1 well, the nitrogen isotopes varied from  $-3\text{‰}$  to  $0\text{‰}$ , while in the Jiangye-1 well, the nitrogen isotopes varied from  $-1\text{‰}$  to  $0\text{‰}$ .

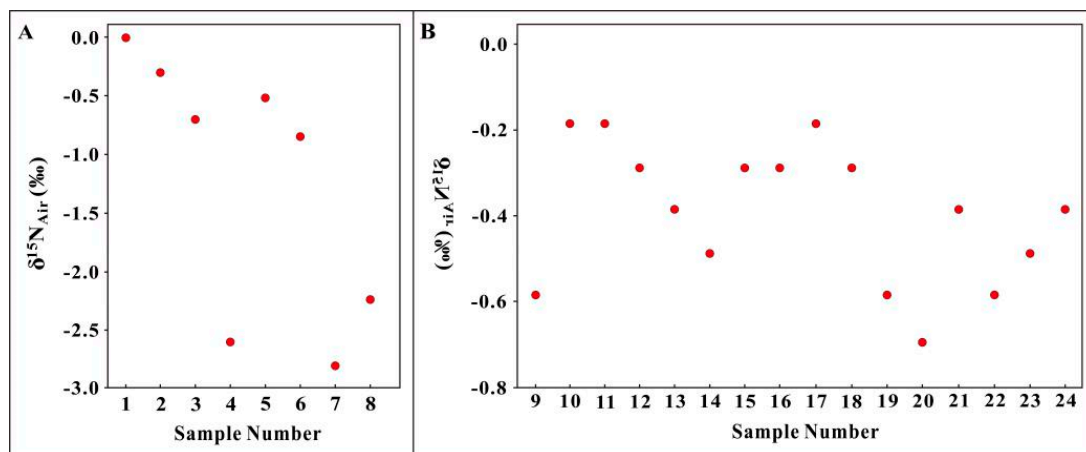


**Figure 3.** Results of nitrogen isotope analysis. (A) Niutitang Formation gas samples in the Youye-1 well; (B) Wangyinpu and Guanyintang Formations gas samples in the Jiangye-1 well. The gas sample information can be seen in Table 1.

Due to different origins, nitrogen from various sources is characterized by different isotopic compositions [17,32,33]. Nitrogen sources, origins, and corresponding isotope characteristics are listed in Table 3, which shows that the source of the nitrogen for the gas samples in the Youye-1 well was organic-matter thermal evolution and the atmosphere, while source of the nitrogen for the gas samples in the Jiangye-1 was the upper mantle, the superdeep crust, and the atmosphere.



## 4.2. Analysis of Nitrogen Derived from the Atmosphere

### 4.2.1. Migration Channels with Permeability Parallel to Stratification Plane

The permeability experiment results and data statistics for the Wangyinpu and Guanyintang Formations shale core from the Jiangye-1 and Jiangye-2 wells and the Longmaxi Formation shale core from the Pengye-1 well are shown in Figures 4 and 5. The experimental results show that due to well-developed stratification planes in the shale, the permeability parallel to the stratification plane was more than 1–40 times greater than the permeability perpendicular to the stratification plane, which means that the gas in the shale strata mainly flowed along the direction parallel to stratification plane.

**Table 3.** Isotope variation characteristics of nitrogen from various sources (Zeng, 2002 and Liu et al., 2006).

Nitrogen Source	Origin	Isotope Characteristics
Atmosphere	Surface water carrying nitrogen	$\delta^{15}\text{N} \approx 0\text{‰}$
Upper mantle and superdeep crust	Produced by various radiation effects and thermal reactions in Earth's core	$\delta^{15}\text{N} \approx -2\text{‰}$ to $+1\text{‰}$
Metamorphism	Generated by high-temperature metamorphism of nitrogenous minerals	$\delta^{15}\text{N} \approx +1\text{‰}$ to $+3.5\text{‰}$
Microbial denitrification	Formed by the interaction between organic matter and biological	$\delta^{15}\text{N} \approx -17\text{‰}$ to $-10\text{‰}$
Deposition		Immature: $\delta^{15}\text{N} \leq 10\text{‰}$
Organic material evolution	Generated in various stages of thermal evolution of organic matter	Mature and high mature: $\delta^{15}\text{N} \approx -10\text{‰}$ to $-1\text{‰}$
		Overmature: $\delta^{15}\text{N} \approx +5\text{‰}$ to $+20\text{‰}$

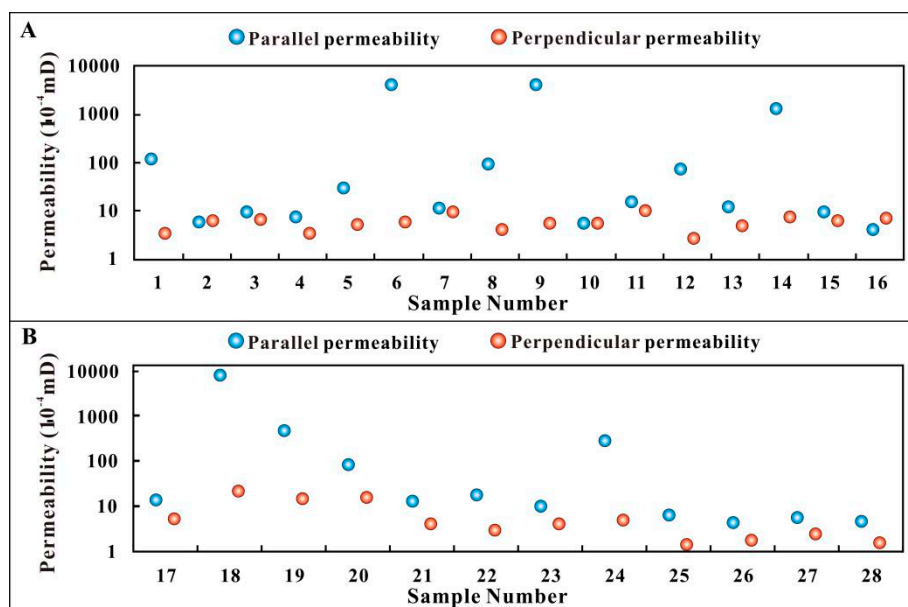


**Figure 4.** Parallel and perpendicular permeability scattergrams. (A) Samples of Wangyinpu and Guanyintang Formations shale from the Jiangye-1 and Jiangye-2 wells; (B) samples of Longmaxi Formation shale from the Pengye-1 well. The sample information can be seen in Table 2.

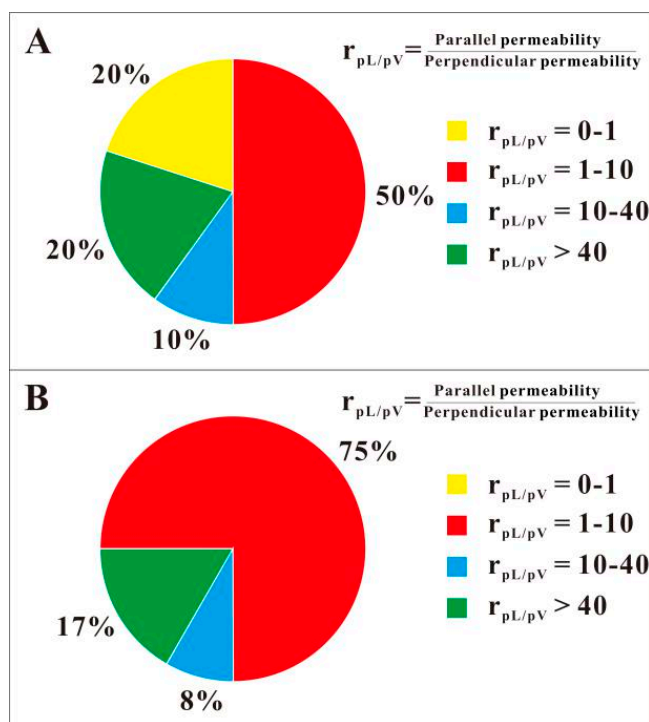


**Figure 5.** Ratio statistics between parallel and perpendicular permeability. (A) Samples of Wangyinpu and Guanyintang Formations shale from the Jiangye-1 and Jiangye-2 wells; (B) samples of Longmaxi Formation shale from the Pengye-1 well. The sample information can be seen in Table 2.

The bedding slip surfaces, known as the detachment layer, often developed microfractures in different directions and higher reflectivity than the shale matrix, resembling a polish from simple shear [34,35]. Through the observation of cores from the Niutitang Formation in the Youye-1 well, the bedding slip surfaces can be found (Figure 6A,B). Similarly, a bedding slip deformation was observed in cores from the Wangyinpu Formation of the Jiangye-1 and Jiangye-2 wells (Figure 6C,D), and obvious interlayer slippage and corrugation occurred in the Pukou profile in the northern part of the Xiuwu Basin (Figure 6E), which indicates that the detachment layers were widely developed at the bottom of the Lower Cambrian in the Xiuwu Basin and Southeast Chongqing region. Because the Xiuwu Basin was subjected to compressive stress in the northeast direction and the Southeast Chongqing region was subjected to compressive stress from the southeast direction and [36–38], the relative slide between the hard Sinian siliceous dolomite and the soft Lower Cambrian organic-rich shale resulted in the formation of detachment layers. The stratification plane was the lateral migration channel of shale gas, while the detachment layers greatly accelerated the process of gas diffusion [39]. In this study, both areas were synclinal geological units, and the target strata in the synclinal wings were both exposed to the ground surface, which provided a pathway for the migration of gases (Figures 7 and 8). Hydrocarbon gases migrated along the detachment layers and the stratification planes from the center of the syncline to the flanks. Meanwhile, the nitrogen gas in the air entered the shale reservoir along the detachment layers and the stratification planes, forming high nitrogen content from the atmosphere.

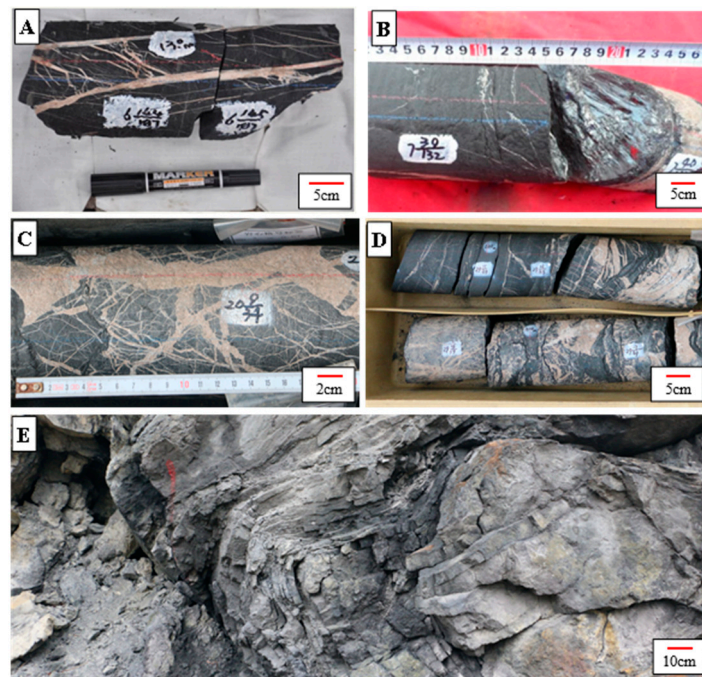


**Figure 6.** Detachment layers developed at the bottom of the Lower Cambrian in cores and field profiles in the Southeast Chongqing region and Xiuwu Basin. (A) Cores from the Niutitang Formation in the Youye-1 well, 3820 m; (B) cores from the Niutitang Formation in the Youye-1 well, 3827 m; (C) cores from the Wangyinpu Formation in the Jiangye-1 well, 2671 m; (D) cores from the Wangyinpu Formation in the Jiangye-2 well, 3130 m; (E) The Wangyinpu Formation in the Pukou profile. The well locations can be seen in Figure 1.

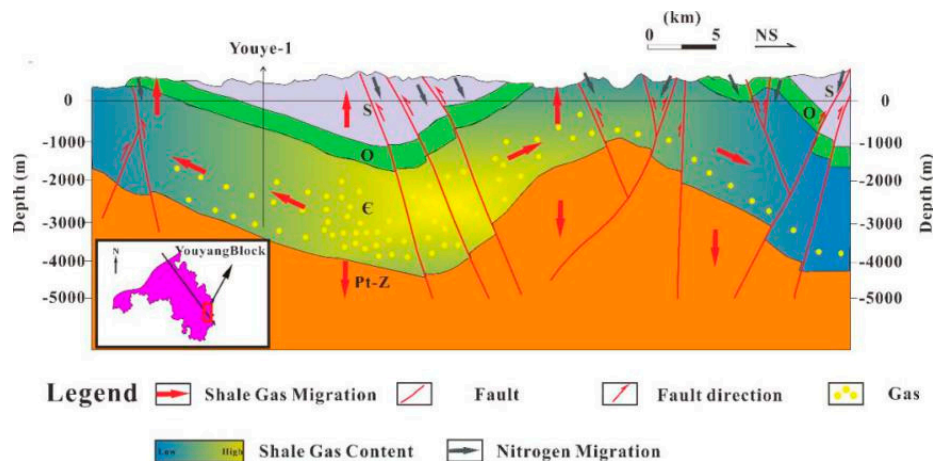


**Figure 7.** Seismic interpretation results for Southeast Chongqing region.

#### 4.2.2. Migration Channels with Perpendicular to Stratification Plane

The Southeast Chongqing region is located in the southeast side of the Sichuan Basin. During the Cretaceous, this region underwent extrusion stress in the southeast direction, which caused the formations to be squeezed and uplifted and produced a large number of thrust faults. According to the results of seismic interpretation, this continuous extrusion was intense, and most of the thrust faults are deep (Figure 7).

Based on the analysis of the tectonic evolution history, during the Early-Middle Jurassic, the Xiuwu Basin developed numerous faults and compressed into a syncline due to the collision and extrusion between the North China and South China plates [37]. During the Late Cretaceous–Paleogene,

the Xiuwu Basin was subjected to tensile action due to the impact of the collision and subduction of the Pacific plate toward the Eurasian plate [38]. Since the Neogene period, the stress on the thrust faults changed from tension to compression again [31,40]. According to the results of seismic interpretation, there were several deep faults in the study area in the vertical direction (Figure 8).

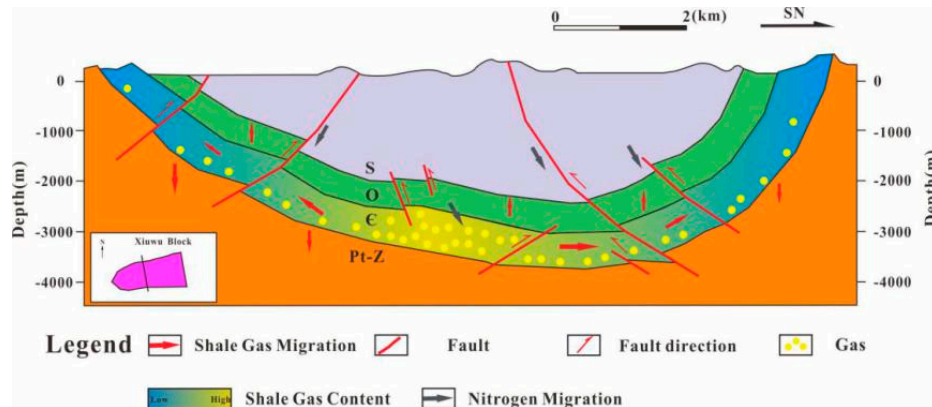


Figure 8. Seismic interpretation results for the Xiuwu Basin.

The development of fractures destroys the seal in the direction perpendicular to the horizontal plane, causing methane and other hydrocarbon gases to escape [41] and the entry of nitrogen from the atmosphere to target layer along the fractures [15]. The fault-opening events happened in the Late Cretaceous–Paleogene in the Xiuwu Basin, and the development of the deep faults in the Southeast Chongqing region accelerated these processes.

#### 4.3. Analysis of Nitrogen Produced in Stages of Organic Matter Evolution

Because of the lack of vitrinite in the Lower Paleozoic, maturity evaluation is usually performed using the equivalent vitrinite reflectance (equal-Ro) calculated from asphalt reflectance [42]. According to the hydrocarbon generation history restored by Zhao et al., 2018 (Figure 9), the Niutitang Formation shale in the Southeast Chongqing region entered high mature stage in the Late Ordovician period [43]. In the Middle Silurian, the shale region entered the overmature stage (equal-Ro > 2.0%). Due to strata uplift, the maturity of organic matter no longer increased and equal-Ro of the shale eventually reached 3.13% to 3.49%, falling into the partial graphitization stage [44,45].

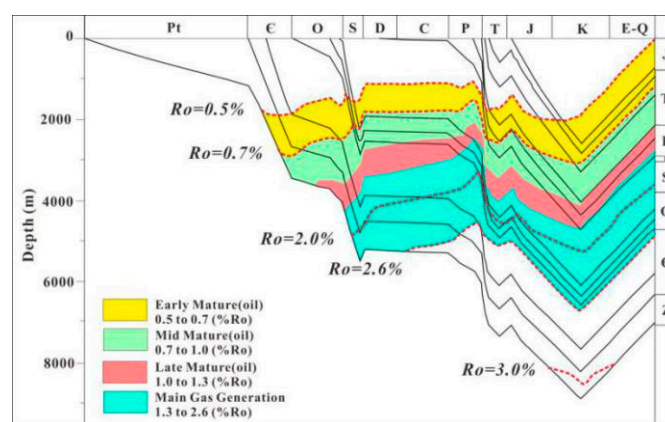
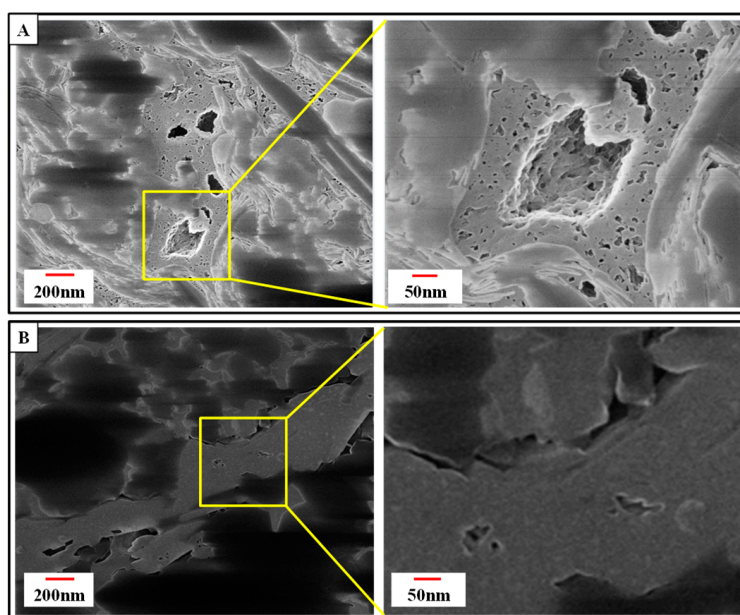


Figure 9. Hydrocarbon generation history in the Southeast Chongqing (modified from Zhao et al., 2018).

Equivalent vitrinite reflectances of shale samples used for FIB observation from the Jiaoye-1 well and Youye-1 well were 2.58% and 3.47% respectively. It was observed that there was nesting



of small pyrobitumen pores in large pores in the shale sample taken from the Longmaxi Formation of the Jiaoye-1 well. These pore development features could increase the organic matter reservoir capacity and the specific surface area (Figure 10A). Only isolated pores were developed in the organic matter pores (OM-pores) in the shale sample taken from the Niutitang Formation of the Youye-1 well, with a small amount and poor reservoir capacity (Figure 10B). When equal-Ro  $>3.0\%$ , the graphitization of organic matter appears [45]. During graphitization, the property of organic matter changes, which compromises the reservoir space, mainly embodied as deformation of the organic matter pore structure and dramatic reduction of pores [46–50]. Organic matter in shale samples from Youye-1 well reaches the graphitization stage. Compared with the Jiaoye-1 well, organic pores in shale samples from the Youye-1 well were poorly developed.



**Figure 10.** Focused ion beam–helium ion microscopy (FIB–HIM) images of organic-rich shale. (A) Organic-rich shale (total organic carbon (TOC) = 4.44%, equal-Ro = 2.58%) of the Longmaxi Formation from the Jiaoye-1 well, 2402 m.; (B) organic-rich shale (TOC = 5.78%, equal-Ro = 3.47%) in the Niutitang Formation from the Youye-1 well, 3811 m. The well locations can be seen in Figure 1.

Organic matter can produce nitrogen in the mature to high mature stage (equal-Ro = 0.7–2.0%), which was adsorbed in the shale organic matter pores [17]. The Lower Cambrian shale of the Youye-1 well went through the mature to high maturity stage and nitrogen was produced in this stage. Due to changes in the nature of the organic matter, ultra-high thermal evolution of organic matter results in an exhaustion situation of generation potential in shale, and the adsorption capacity of organic matter for methane is reduced [43,46,47]. The result is that the methane in the pores escaped to shallower layers or the atmosphere, and nitrogen with strong adsorption capacity was retained, which finally caused the characteristics of low hydrocarbon and high nitrogen.

#### 4.4. Analysis of Nitrogen Derived from Upper Mantle and Superdeep Crust

Krooss et al. (1995) concluded that nitrogen originating from the superdeep zone of crust and upper mantle zone is generally concentrated in volcanic activity zones, while in other regions, the nitrogen content is actually very low [51]. According to the regional structural analysis, the Niutitang Formation in the Youyang-1 well was not directly affected by volcanic activity, while the Xiuwu Basin was influenced by magmatism during the Jurassic, and remnants of Jurassic eruptive rocks are also present on both sides of the basin. The magmatic activity in the Xiuwu Basin led to changes in the ancient heat flow. The values of the ancient heat flow in the Xiuwu Basin have undergone great changes since the

Early Cambrian, as shown in Figure 11. The value of the ancient heat flow between the Cambrian and Late Triassic (543–199 Ma) increased slowly from 50 mW/m<sup>2</sup> to 54 mW/m<sup>2</sup>. During the Jurassic (199–137 Ma), magmatism began to become active in the Xiuwu Basin due to the collision between the North China and South China plates, causing a sharp increase in the value of the heat flow to 71 mW/m<sup>2</sup>. During the Early Cretaceous (137–96 Ma), the value of the heat flow decreased gradually. From the Late Cretaceous to the Paleogene (96–23.3 Ma), as the stress changed from compression to tension, the value increased to 62 mW/m<sup>2</sup>, and then it gradually cooled to the present [52]. The magmatic activity carried nitrogen originating from the superdeep zone of crust and upper mantle into zones near the basin basement. Nitrogen was volatilized and moved into the Wangyinpu and Guanyintang Formation shale reservoir through the fault during the cooling down of magma [53]. Therefore, based on the above analysis, the nitrogen in the Jiangye-1 well was derived from the superdeep zone of crust and the upper mantle zone, while there is no evidence that these were the sources of nitrogen in the Youye-1 well.

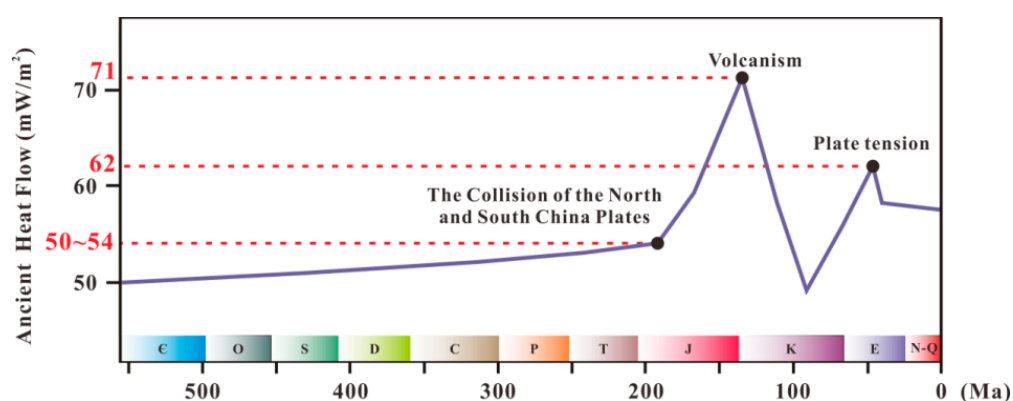


Figure 11. Historical map of ancient heat flow in the Xiuwu Basin (modified from Li et al., 2016).

#### 4.5. Destruction Model for Shale Gas Reservoirs in Areas of Active Plate Movement

From the above analysis, there are three main sources of nitrogen in shale reservoirs under complex tectonic settings: From the atmosphere carried by surface water, produced in mature and high mature stages of organic matter evolution, from the superdeep zone of crust, and from the upper mantle zone. Due to strong tectonic activity, it is easier for the strata to form channels for gas migration. In the lateral direction, stratification planes and detachment layers became the main channels for atmospheric nitrogen into shale reservoirs and methane dissipation, while in the vertical direction, faults are the main channels for entry of nitrogen and methane dissipation, such as the development of deep faults in the Southeast Chongqing region and the opening of the Late Cretaceous–Paleogene faults in the Xiuwu Basin.

Based on nitrogen isotope analysis results, the nitrogen in the southeastern Chongqing region not only comes from the atmosphere, but also from the thermal evolution process of organic matter. On the one hand, when the maturity of organic matter reaches the stage of graphitization, its brittleness changes and the OM-pores collapse under the overlying pressure, resulting in fewer pores, smaller pore size, and bad storage capacity. Then, the strata begin to uplift, causing the development of faults, denudation of the overlying strata, and the escape of hydrocarbon gas. On the other hand, since the adsorption capacity of nitrogen is stronger than methane, part of the nitrogen produced during the thermal evolution of organic matter is adsorbed on the surface of OM-pores and retained in shale reservoirs [54,55]. In summary, detachment layers at the bottom of the Lower Cambrian in the lateral direction, shale stratification planes, vertical deep faults, and thermal evolution of organic matter are the dominant causes of low contents of hydrocarbons and high contents of nitrogen in shale gas from the Southeast Chongqing region (Figure 12A).

Based on nitrogen isotope analysis results, the nitrogen in the Xiuwu Basin comes not only from the atmosphere, but also from the superdeep zone of crust and upper mantle zone. Combined with



previous studies [31], the Xiuwu Basin is not far from the junction of the South China and North China plates, which made the basin easily affected by magmatic activity caused by the collision between the two plates. On the one hand, the magmatism carried nitrogen originating from the upper mantle and superdeep crust into the Lower Cambrian shale reservoir, which caused an increase in nitrogen content. On the other hand, with the heat flow value increasing continuously, abnormally high temperatures not only made the Wangyinpu and Guanyintang Formation shale enter the graphitization stage, but also reduced the adsorption capacity of shale gas. Both of these processes promoted shale gas loss. Therefore, the detachment layers at the bottom of the Lower Cambrian, shale stratification planes which extensively developed faults in the vertical direction, and magmatism during the Jurassic are the reasons for the low contents of hydrocarbons and high contents of nitrogen and in shale gas from the Xiuwu Basin (Figure 12B).

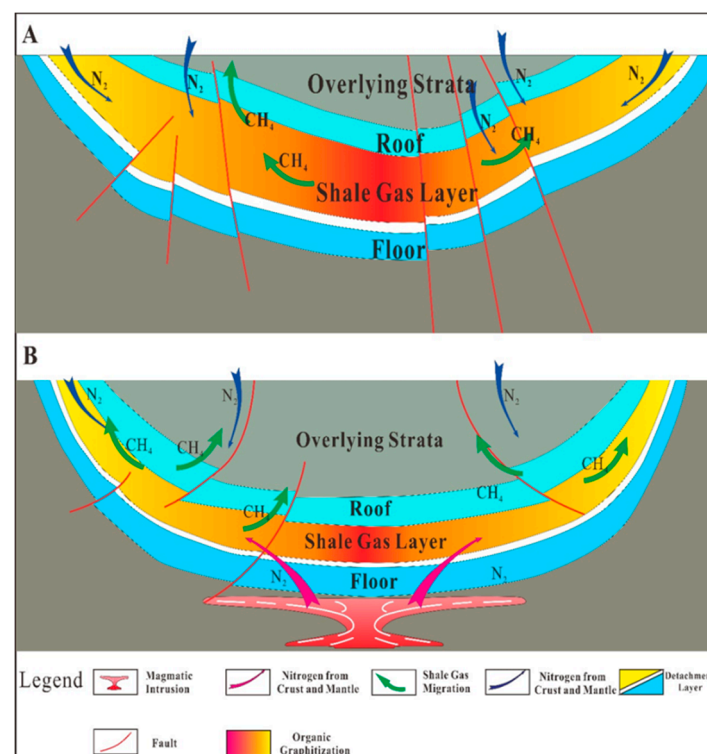


**Figure 12.** Destruction model for shale gas reservoirs in areas of active plate movement: (A) Southeast Chongqing region in the Upper Yangtze area; (B) Xiuwu Basin in the Lower Yangtze area.

The Xiuwu Basin and Southeast Chongqing region are representative blocks within the complex tectonic backgrounds of the Upper and Lower Yangtze areas. This model can be used to explain the occurrence of low contents of hydrocarbon and high contents of nitrogen phenomena in the Upper and Lower Yangtze areas and in tectonically active regions. Due to the limitation of oil and gas production technology, such shale gas reservoirs cannot achieve effective commercial development. In shale gas exploration, the location of wells in such models should be avoided.

## 5. Conclusions

- (1) The main sources of nitrogen in the Southeast Chongqing region is the thermal evolution of organic matter and atmosphere. Large-scale tectonic events in the research area caused extensive thrust faults and detachment layers, which destroyed the already-formed shale gas reservoir. The shale stratification planes and partial graphitization of organic matter accelerated the methane dissipation. In the meantime, nitrogen originating from the atmosphere intruded into

the shale reservoir and mixed with nitrogen produced by thermal evolution of organic matter in the reservoir.

- (2) The main sources of nitrogen in Xiuwu Basin are the superdeep crust, upper mantle, and atmosphere. Intensive tectonic activities and magmatism in the research area promoted the development of thrust faults and detachment layers and resulted in a tremendous loss of gaseous hydrocarbons. Meanwhile, nitrogen originating from the atmosphere and mantle intruded into the shale reservoir. Besides, the shale stratification planes also provided migration channels for nitrogen and methane.
- (3) The destruction models of shale gas reservoir in areas of active plate movement were summarized. These models can be used to explain the phenomena of low contents of hydrocarbon and high contents of nitrogen in the Yangtze regions. In shale gas exploration, the locating of wells in such models should be avoided.

**Author Contributions:** Conceptualization, X.W.; Data curation, K.Z., M.W., T.L., and X.X.; Formal analysis, X.W., and K.Z.; Funding acquisition, Z.J.; Methodology, X.W., K.Z., M.W., and W.W.; Project administration, Z.J.; Visualization, X.W., Y.H., and X.L.; Writing—original draft, X.W.; Writing—review and editing, X.W., Z.J., K.Z., M.W., Z.X., and Q.W. All authors have read and agreed to the published version of the manuscript.

**Funding:** This study was supported by the Petro China Southwest Oil & Gasfield Company Science Foundation (No. XNS25JS2018-38), the National Science and Technology Major Project (No. 2017ZX05035-002), the Project of Chongqing Institute of Geology and Mineral Resources “Study on influence factors of gas content difference distribution in shale” (No. CSTC2017XJL90010), the open fund of the Sinopec Key Laboratory of Shale Oil/Gas Exploration and Production Technology, and the National Natural Science Foundation of China (No. 41472112 and No. 41728004).

**Acknowledgments:** We sincerely appreciate all reviewers and the handling editor for their critical comments and constructive suggestions.

**Conflicts of Interest:** The authors declare no conflict of interest.

## References

1. Curtis, J.B. Fractured shale-gas systems. *AAPG Bull.* **2002**, *86*, 1921–1938.
2. Montgomery, S.L.; Jarvie, D.M.; Bowker, K.A.; Pollastro, R.M. Mississippianbarnett shale, fort Worth Basin, north-central Texas: Gas-shale play with multitrillion cubic foot potential. *AAPG Bull.* **2005**, *89*, 155–175. [[CrossRef](#)]
3. Warlick, D. Gas shale and CBM development in North America. *Oil Gas Financ. J.* **2006**, *3*, 1–5.
4. Zhu, H.; Deng, J.; Jin, X.; Hu, L.; Luo, B. Hydraulic Fracture Initiation and Propagation from Wellbore with Oriented Perforation. *Rock. Mech. Rock. Eng.* **2015**, *48*, 585–601. [[CrossRef](#)]
5. Zhu, H.; Jin, X.; Guo, J.; An, F.; Wang, Y. Coupled flow, stress and damage modelling of interactions between hydraulic fractures and natural fractures in shale gas reservoirs. *Int. J. Oil Gas Coals Technol.* **2016**, *13*, 359–390. [[CrossRef](#)]
6. Wu, M.; Ding, M.; Yao, J.; Xu, S.; Li, L.; Li, X. Pressure transient analysis of multiple fractured horizontal well in composite shale gas reservoirs by boundary element method. *J. Pet. Sci. Eng.* **2018**, *162*, 84–101. [[CrossRef](#)]
7. Czarnota, R.; Stopa, J.; Janiga, D.; Kosowski, P.; Wojnarowski, P. Semianalytical horizontal well length optimization under pseudosteady-state conditions. In Proceedings of the 2018 2nd International Conference on Smart Grid and Smart Cities (ICSGSC), Kuala Lumpur, Malaysia, 12–14 August 2018; IEEE: Piscataway, NJ, USA, 2019; pp. 68–72.
8. Yang, H.; Zhang, X.; Chen, M.; Wu, J.; Zhang, J.; You, C. Optimization of the key geological target parameters of shale-gas horizontal wells in the Changning Block, Sichuan Basin. *Nat. Gas Ind. B* **2016**, *3*, 571–576. [[CrossRef](#)]
9. Guo, X.; Hu, D.; Li, Y.; Wei, Z.; Wei, X.; Liu, Z. Geological factors controlling shale gas enrichment and high production in fuling shale gas field. *Petrol. Explor. Dev.* **2017**, *44*, 481–491. [[CrossRef](#)]
10. Chen, A. Nitrogen as an index of oil-gas preservation conditions in marine strata. *Petrol. Explor. Dev.* **2005**, *27*, 85–89, (In Chinese with English abstract).

11. Chen, J.; Zhu, Y. The origin of molecular nitrogen in natural gas and geochemical characters of molecular nitrogen in natural gas from east part of Tarim Basin. *Nat. Gas Geosci.* **2003**, *14*, 172–176, (In Chinese with English abstract).
12. Li, J.; Li, Z.; Wang, D.; Li, J.; Cheng, H.; Xie, Z.; Wang, X.; Xie, Q. Geochemical characteristics and N<sub>2</sub> source of nitrogen riched natural gas in Tarim Basin. *Acta Pet. Sin.* **2013**, *34*, 102–111, (In Chinese with English abstract).
13. He, J.; Yan, W.; Cui, J. Nitrogen gas source tracking and distinguishing in margin basins, northern South China Sea. *Mar. Orig. Pet. Geol.* **2012**, *17*, 85–89, (In Chinese with English abstract).
14. Jiao, W.; Wang, S.; Cheng, L.; Luo, Q.; Fang, G. The reason of high nitrogen content and low hydrocarbon content of shale gas from the Lower Cambrian Niutitang Formation in southeast Chongqing. *Nat. Gas Geosci.* **2017**, *28*, 1882–1890, (In Chinese with English abstract).
15. Maksimov, S.N.; Müller, E.; Botneva, T.A.; Goldbecher, K.; Zor'kin, L.M.; Pankina, R.G. Origin of high-nitrogen gas pools. *Int. Geol. Rev.* **1976**, *18*, 551–556. [[CrossRef](#)]
16. Liu, Q.; Jin, Z.; Chen, J.; Krooss, B.M.; Qin, S. Origin of nitrogen molecules in natural gas and implications for the high risk of N<sub>2</sub> exploration in Tarim basin, NW China. *J. Petrol. Sci. Eng.* **2012**, *81*, 112–121. [[CrossRef](#)]
17. Liu, Q.; Liu, W.; Krooss, B.M.; Wang, W.; Dai, J. Advances in nitrogen geochemistry of natural gas. *Nat. Gas Geosci.* **2006**, *17*, 120–124, (In Chinese with English abstract).
18. Zhao, W.; Li, J.; Yang, T.; Wang, S.; Huang, J. Geological difference and its significance of marine shale gases in South China. *Petrol. Explor. Dev.* **2016**, *43*, 547–559. [[CrossRef](#)]
19. Kang, J.; Lin, X.; Yu, Q.; Tian, J.; Men, Y.; Yan, J.; Lin, J.; Sun, Y. Shale gas enrichment conditions in complex geological structure areas: A case study in the front margin of Daba Mountain. *Pet. Geol. Exp.* **2017**, *39*, 437–443, (In Chinese with English abstract).
20. Hu, M.; Huang, W.; Li, J. Effects of structural characteristics on the productivity of shale gas wells: A case study on the Jiaoshiha Block in the Fuling Shale gas field, Sichuan Basin. *Nat. Gas Ind.* **2017**, *37*, 31–39, (In Chinese with English abstract). [[CrossRef](#)]
21. Li, Z.; Zhang, L.; Powell, C.M. South China in Rodinia: Part of the missing link between Australia-east Antarctica and Laurentia? *Geology* **1995**, *23*, 407–410. [[CrossRef](#)]
22. Li, Z.; Li, X.; Zhou, H.; Kinny, P.D. Grenvillian continental collision in South China: New SHRIMP U-Pb zircon results and implications for the configuration of Rodinia. *Geology* **2002**, *30*, 163–166. [[CrossRef](#)]
23. Wang, J.; Li, Z. History of Neoproterozoic rift basins in South China: Implications for Rodinia break-up. *PreCambrian Res.* **2003**, *122*, 141–158. [[CrossRef](#)]
24. Zhu, G.; Zhang, S.; Liang, Y.; Ma, Y.; Dai, J.; Jian, L. The characteristics of natural gas in sichuan basin and its sources. *Earth Sci. Front.* **2006**, *13*, 234–248.
25. Zhang, K.; Jiang, Z.; Yin, L.; Gao, Z.; Wang, P.; Song, Y.; Jia, C.; Liu, W.; Liu, T.; Xie, X.; et al. Controlling functions of hydrothermal activity to shale gas content-taking lower Cambrian in Xiuwu Basin as an example. *Mar. Petrol. Geol.* **2017**, *85*, 177–193. [[CrossRef](#)]
26. Wojnarowski, P.; Czarnota, R.; Janiga, D.; Stopa, J. Novel liquid-gas corrected permeability correlation for dolomite formation. *Int. J. Rock Mech. Min. Sci.* **2018**, *112*, 11–15. [[CrossRef](#)]
27. Al-Jabri, R.A.; Al-Maamari, R.S.; Wilson, O.B. Klinkenberg-corrected gas permeability correlation for Shuaiba carbonate formation. *J. Pet. Sci. Eng.* **2015**, *131*, 172–176. [[CrossRef](#)]
28. Tanikawa, W.; Shimamoto, T. Comparison of Klinkenberg-corrected gas permeability and water permeability in sedimentary rocks. *Int. J. Rock Mech. Min. Sci.* **2009**, *46*, 229–238. [[CrossRef](#)]
29. Achang, M.; Pashin, J.C.; Cui, X. The influence of particle size, microfractures, and pressure decay on measuring the permeability of crushed shale samples. *Int. J. Coal Geol.* **2017**, *183*, 174–187. [[CrossRef](#)]
30. He, X.; Gao, Y.; Tang, X.; Zhang, P.; He, G. Analysis of major factors controlling the accumulation in normal pressure shale gas in the southeast of Chongqing. *Nat. Gas Ind.* **2017**, *28*, 654–664, (In Chinese with English abstract).
31. Zhang, K.; Jia, C.; Song, Y.; Jiang, S.; Jiang, Z.; Wen, M.; Huang, Y.; Liu, X.; Jiang, T.; Peng, J.; et al. Analysis of Lower Cambrian shale gas composition, source and accumulation pattern in different tectonic backgrounds: A case study of Weiyuan Block in the Upper Yangtze region and Xiuwu Basin in the Lower Yangtze region. *Fule* **2020**, *263*, 115978. [[CrossRef](#)]
32. Schimmelmann, A.; Lis, G.P.; Böttcher, M.E.; Bouillon, S. Nitrogen isotopic exchange during maturation of organic matter. *Org. Geochem.* **2010**, *41*, 63–70. [[CrossRef](#)]

33. Zeng, Z. Genetic type of nitrogen gas in sedimentary basins in China. *Nat. Gas Geosci.* **2002**, *13*, 29–33, (In Chinese with English abstract).
34. Zhu, H.; Ju, Y.; Huang, C.; Han, K.; Qi, Y.; Shi, M.; Yu, K.; Feng, H.; Li, W.; Ju, L.; et al. Pore structure variations across structural deformation of Silurian Longmaxi Shale: An example from the Chuandong Thrust-Fold Belt. *Fuel* **2019**, *241*, 914–932. [\[CrossRef\]](#)
35. Aydin, M.G.; Terry Engelder, T. Revisiting the Hubbert–Rubey pore pressure model for overthrust faulting: Inferences from bedding-parallel detachment surfaces within Middle Devonian gas shale, the Appalachian Basin, USA. *J. Struct. Geol.* **2014**, *69*, 519–537. [\[CrossRef\]](#)
36. Xu, Z.; Jiang, S.; Yao, G.; Liang, X.; Xiong, S. Tectonic and depositional setting of the lower Cambrian and lower Silurian marine shales in the Yangtze Platform, South China: Implications for shale gas exploration and production. *J. Asian Earth Sci.* **2019**, *170*, 1–19. [\[CrossRef\]](#)
37. Mei, L.; Deng, D.; Shen, C.; Liu, Z. Tectonic Dynamics and Marine Hydrocarbon Accumulation of Jiangnan-Xuefeng Uplift. *Geol. Sci. Technol. Inf.* **2012**, *31*, 85–93, (In Chinese with English abstract).
38. Wo, Y.; Zhou, Y.; Xiao, K. The burial history and models for hydrocarbon generation and evolution in the marine strata in Southern China. *Sediment. Geol. Tethyan Geol.* **2007**, *27*, 94–100.
39. Liu, A.; Ou, W.; Huang, H.; Wei, K.; Li, H.; Chen, X. Significance of paleo-fluid in the Ordovician–Silurian detachment zone to the preservation of shale gas in western Hunan–Hubei area. *Nat. Gas Ind. B* **2018**, *5*, 565–574. [\[CrossRef\]](#)
40. Wang, P.; Jiang, Z.; Ji, W.; Zhang, C.; Yuan, Y.; Chen, L.; Yin, L. Heterogeneity of intergranular, intraparticle and organic pores in Longmaxi shale in Sichuan Basin, South China: Evidence from SEM digital images and fractal and multifractal geometries. *Mar. Pet. Geol.* **2016**, *72*, 122–138. [\[CrossRef\]](#)
41. Zhang, K.; Jiang, Z.; Xie, X.; Gao, Z.; Liu, T.; Yin, L.; Jia, C.; Song, Y.; Shan, C.; Wu, Y.; et al. Lateral Percolation and Its Effect on Shale Gas Accumulation on the Basis of Complex Tectonic Background. *Geofluids* **2018**, *2018*, 5195469. [\[CrossRef\]](#)
42. Schoenherr, J.; Littke, R.; Urai, J.L.; Kukla, P.A.; Rawahi, Z. Polyphase thermal evolution in the Infra-Cambrian Ara Group (South Oman Salt Basin) as deduced by maturity of solid reservoir bitumen. *Org. Geochem.* **2007**, *38*, 1293–1318. [\[CrossRef\]](#)
43. Zhao, W.; Jing, T.; Xiong, X.; Wu, B.; Zhou, Y. Graphitization Characteristics of Organic Matter in Marine-Facies Shale: A case study of Niutitang Formation in Southeast Chongqing region. *Geol. Sci. Technol. Inf.* **2018**, *37*, 183–191, (In Chinese with English abstract).
44. Sun, M.; Yu, B.; Hu, Q.; Chen, S.; Xia, W.; Ye, R. Nanoscale pore characteristics of the Lower Cambrian Niutitang Formation Shale: A case study from Well Yuke #1 in the Southeast of Chongqing, China. *Int. J. Coal Geol.* **2016**, *154*, 16–29.
45. Tang, X.; Jiang, Z.; Jiang, S.; Wang, P.; Xiang, C. Effect of organic matter and maturity on pore size distribution and gas storage capacity in high-mature to post-mature shales. *Energy Fuel* **2017**, *30*, 8985–8996. [\[CrossRef\]](#)
46. Curtis, M.E.; Cardott, B.J.; Sondergeld, C.H.; Rai, C.S. Development of organic porosity in the Woodford Shale with increasing thermal maturity. *Int. J. Coal Geol.* **2012**, *103*, 26–31. [\[CrossRef\]](#)
47. Ji, W.; Song, Y.; Jiang, Z.; Wang, X.; Bai, Y.; Xing, J. Geological controls and estimation algorithms of lacustrine shale gas adsorption capacity: A case study of the Triassic strata in the Southeastern Ordos Basin, China. *Int. J. Coal. Geol.* **2014**, *134–135*, 61–73. [\[CrossRef\]](#)
48. Ji, W.; Song, Y.; Jiang, Z.; Meng, M.; Liu, Q.; Chen, L.; Wang, P.; Gao, F.; Huang, H. Fractal characteristics of Nano-pores in the lower Silurian Longmaxi shales from the upper Yangtze Platform, South China. *Int. J. Coal Geol.* **2016**, *78*, 88–98. [\[CrossRef\]](#)
49. Wang, S.; Zhang, Z.; Dong, D.; Wang, Y.; Li, X.; Hu, J.; Huang, J.; Guan, Q. Microscopic pore structure and reasons making reservoir property weaker of Lower Cambrian Qiongzhusi shale, Sichuan Basin, China. *Nat. Gas Geosci.* **2016**, *27*, 1619–1628, (In Chinese with English abstract).
50. Wang, Y.; Dong, D.; Cheng, X.; Huang, J.; Wang, S.; Wang, S. Electric property evidences of the carbonification of organic matters in marine shales and its geologic significance: A case of the Lower Cambrian Qiongzhusi Shale in southern Sichuan Basin. *Nat. Gas Ind.* **2014**, *34*, 1–7, (In Chinese with English abstract). [\[CrossRef\]](#)
51. Krooss, B.M.; Littke, R.; Müller, B.; Frielingdorf, J.; Schwochau, K.; Idiz, E.F. Generation of nitrogen and methane from sedimentary organic matter: Implications on the dynamics of natural gas accumulations. *Chem. Geol.* **1995**, *126*, 291–318. [\[CrossRef\]](#)

52. Li, Y.; Jiang, Z.; Liu, W.; Huang, R.; Zhang, K.; Cheng, S.; Gao, Z.; Gao, F.; Xiong, F. The Effect of the Tectonic Thermal Evolution History to Gas Content of Lower Cambrian Shales at Xiuwu Basin. *Sci. Technol. Eng.* **2016**, *16*, 44–51, (In Chinese with English abstract).
53. Xu, S.; Zheng, G.; Zheng, J.; Zhou, S.; Shi, P. Mantle-derived helium in foreland basins in Xinjiang, Northwest China. *Tectonophysics* **2017**, *694*, 319–331. [[CrossRef](#)]
54. Aroua, M.K.; Daud, W.M.A.W.; Yin, C.Y.; Adinata, D. Adsorption capacities of carbon dioxide, oxygen, nitrogen and methane on carbon molecular basket derived from polyethyleneimine impregnation on microporous palm shell activated carbon. *Sep. Purif. Technol.* **2008**, *62*, 609–613. [[CrossRef](#)]
55. Li, J.; Yan, X.; Wang, W.; Zhang, Y.; Yin, J.; Lu, S.; Chen, F.; Meng, Y.; Zhang, X.; Chen, X.; et al. Key factors controlling the gas adsorption capacity of shale: A study based on parallel experiments. *Appl. Geochem.* **2015**, *58*, 88–96. [[CrossRef](#)]



© 2020 by the authors. Licensee MDPI, Basel, Switzerland. This article is an open access article distributed under the terms and conditions of the Creative Commons Attribution (CC BY) license (<http://creativecommons.org/licenses/by/4.0/>).